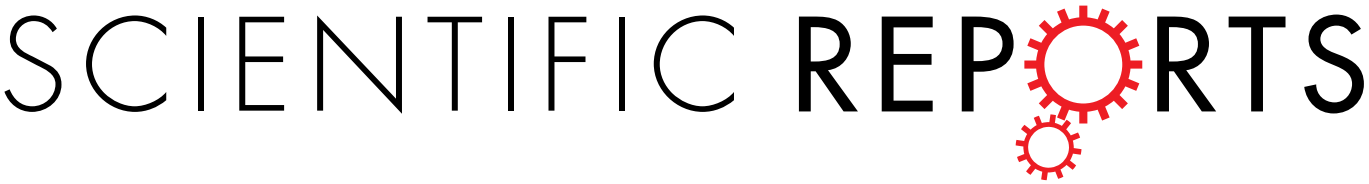

OPEN

Parity Deformed Jaynes-Cummings Model: "Robust Maximally Entangled States"

Received: 04 May 2016
Accepted: 28 October 2016
Published: 05 December 2016

A. Dehghani[1], B. Mojaveri[2], S. Shirin[1] & S. Amiri Faseghandis[2]

The parity-deformations of the quantum harmonic oscillator are used to describe the generalized Jaynes-Cummings model based on the λ-analog of the Heisenberg algebra. The behavior is interestingly that of a coupled system comprising a two-level atom and a cavity field assisted by a continuous external classical field. The dynamical characters of the system is explored under the influence of the external field. In particular, we analytically study the generation of robust and maximally entangled states formed by a two-level atom trapped in a lossy cavity interacting with an external centrifugal field. We investigate the influence of deformation and detuning parameters on the degree of the quantum entanglement and the atomic population inversion. Under the condition of a linear interaction controlled by an external field, the maximally entangled states may emerge periodically along with time evolution. In the dissipation regime, the entanglement of the parity deformed JCM are preserved more with the increase of the deformation parameter, i.e. the stronger external field induces better degree of entanglement.

The Jaynes-Cummings model (JCM) which is used extensively in quantum optics describes the interaction of a single quantized radiation field with a two-level atom. The solvability and applications of this model has long been discussed[1,2]. This simple model describes various quantum mechanical phenomena, for example, Rabi oscillations[2,3], collapse and revivals of the atomic population inversion[4] and entanglement between atom and field[5]. Specifically, it plays an important role in recent quantum information processing[6–11]. Furthermore, JCM is one of the several possible schemes for producing the nonclassical states[12–15]. The dynamics predicted by JCM have been proven in experiments with Rydberg atom in high quality cavities[16]. Since JCM is an ideal model in quantum optics, its various extensions such as intensity dependent coupling, two photons or multi-photon transitions, two- or three- cavity modes for three-level atoms and the Tavis-Cummings model have been proposed[17,18]. In 1984, Sukumer and Buck studied the above mentioned models by using algebraic operator methods[19]. On the other hand, the supergroup theoretical approach to JCM leads to the exact solvability of this model and the representation theory of super-algebras[20]. More recently, a lot of researchers have found that the ordinary creation and annihilation operators in JCM may be replaced by the q-deformed partners, namely, the q-deformed JCM[21]. Later on, JCM has been adopted with a Kerr nonlinearity within the framework of f-oscillator formalism[22]. Furthermore, the investigations of a class of shape-invariant bound state problem, which represents a two-level system, leads to the generalized JCM[23].

In addition to the above -cited generalizations, in recent years, a lot of interest has been given to to the extension of the boson oscillator algebra. One of the most interesting cases which is not related to the q or f-calculus is R-deformed Heisenberg algebra (RDHA). Such generalized schemes naturally lead to the concept of para-fields and para-statistics[18–36]. The same RDHA was also used for solving the quantum mechanical Calogero model or pseudo harmonic oscillator (PHO)[37–41]. Recently, this algebra has been employed for bosonization of super-symmetric quantum mechanics[41–43] and for describing anyons in $(2+1)$[42,44] and $(l+1)$ dimensions[45,46]. All the applications as well as the para-bosonic constructions[32,33] have used infinite-dimensional unitary representations of RDHA. According to Wigner's new quantization method, the RDHA is raised as a unital algebra by the generators $\{1, \mathfrak{a}, \mathfrak{a}^{\dagger}, \hat{R}\}$, which satisfy the (anti-) commutation relations

[1]Department of Physics, Payame Noor University, P.O. Box 19395-3697, Tehran, I.R. of Iran. [2]Department of Physics, Azarbaijan Shahid Madani University, P.O. Box 51745-406, Tabriz, Iran. Correspondence and requests for materials should be addressed to A.D. (email: alireza.dehghani@gmail.com) or B.M. (email: bmojaveri@azaruniv.ac.ir) or S.S. (email: siminshirin2000@gmail.com)

$$[\mathfrak{a}, \mathfrak{a}^\dagger] = 1 + 2\lambda\hat{R}, \{\hat{R}, \mathfrak{a}\} = \{\hat{R}, \mathfrak{a}^\dagger\} = 0. \tag{1}$$

Here, $\lambda \in \mathbb{R}$ is called Wigner's deformation parameter and $\hat{R}$ is a parity operator with the following properties

$$\hat{R}^2 = I, \hat{R}^\dagger = \hat{R}^{-1} = \hat{R}, \tag{2}$$

This acts in the Hilbert space of eigenfunctions as follows

$$\hat{R}|n\rangle = (-1)^n|n\rangle, \tag{3}$$

which means that $\hat{R}$ commutes with number operator $\hat{N}$ that includes the eigenvector $|n\rangle$, such that $\hat{N}|n\rangle = n|n\rangle$. The number operator $\hat{N}$ is in general different from the product $\mathfrak{a}^\dagger\mathfrak{a}$, and is postulated to satisfy the following relations:

$$[\hat{N}, \mathfrak{a}] = -\mathfrak{a}, [\hat{N}, \mathfrak{a}^\dagger] = \mathfrak{a}^\dagger, \tag{4}$$

$$\mathfrak{a}^\dagger\mathfrak{a} = \hat{N} + \lambda(1 - \hat{R}), \tag{5}$$

which provide us with the following irreducible representation of the RDHA

$$\mathfrak{a}|2n\rangle = \sqrt{2n}|2n - 1\rangle, \mathfrak{a}|2n + 1\rangle = \sqrt{2n + 2\lambda + 1}|2n\rangle, \tag{6}$$

$$\mathfrak{a}^\dagger|2n\rangle = \sqrt{2n + 2\lambda + 1}|2n + 1\rangle, \mathfrak{a}^\dagger|2n + 1\rangle = \sqrt{2n + 2}|2n + 2\rangle. \tag{7}$$

The explicit differential forms of the generators $\mathfrak{a}$, $\mathfrak{a}^\dagger$ in terms of the well known annihilation and creation operators a, $a^\dagger$ are obtained[37] as follows:

$$\mathfrak{a} = \frac{1}{\sqrt{2}}\left(\frac{d}{dx} + x - \frac{\lambda}{x}\hat{R}\right) = a - \frac{\lambda}{\sqrt{2}x}\hat{R}, \tag{8}$$

$$\mathfrak{a}^\dagger = \frac{1}{\sqrt{2}}\left(-\frac{d}{dx} + x + \frac{\lambda}{x}\hat{R}\right) = a^\dagger + \frac{\lambda}{\sqrt{2}x}\hat{R}, \tag{9}$$

which provide us with the coordinate representation for the position $\hat{x}$ and its $\lambda-$deformed canonical pair $\hat{p}$ as

$$\hat{x} = \frac{\mathfrak{a} + \mathfrak{a}^\dagger}{\sqrt{2}}, \tag{10}$$

$$\hat{p} = \frac{\mathfrak{a} - \mathfrak{a}^\dagger}{i\sqrt{2}} = -i\frac{d}{dx} + i\frac{\lambda}{x}\hat{R}. \tag{11}$$

It is evident that the above representation is really different from the f- deformed realization of the Heisenberg algebra[47]. Therefore, the introduced RDHA in (1) can be considered as a new deformation of the simple harmonic oscillator with significant features in quantum optics[48,49].

Due to the physical significance of the deformed JCM in quantum optics on the one hand, and the central role of the parity operator in the theory of deformation on the other hand, we then generalize the well-known JCM to a parity deformed-Hermitian case in terms of parity deformed boson operators which are not related to the q or f-deformation. It should be noted that the parity deformed JCM introduced here could be compared, with a major difference, to what has been already discussed in other studies as the q-, f-deformed JCM and so on. It is one of the most interesting cases of the parity operator $\hat{R}$ appeared in the context of quantization schemes generalizing bosonic commutation relations. These Hermitian operators arise from a special deformation of canonical bosonic commutation relations, allowing us a mathematically rigorous treatment of our deformed interaction Hamiltonian, extraction of the energy spectrum, and the corresponding eigen-vectors. Preparing the initial field in the $\lambda-$ deformed cat states, we investigate the collapse and revival phenomena in the Rabi oscillations of the atomic inversion.

Considering the experimental realization, interaction with the environment is an unavoidable feature of real quantum systems. Dissipation phenomenon of energy into the environment is the main feature of such real systems which leads to the loss of entanglement generated in those systems. Some scholars have studied this subject and found interesting phenomena such as entanglement revival[50], entanglement sudden death[51,52] and sudden change for quantum discord[53]. The description of dissipative systems Hamiltonian is a polemic topic in the literature[54,55]. The dissipative systems can be studied in a phenomenological way in which a closed system formed by the cavity including its environment is considered. This larger system is therefore closed, and it is possible to apply quantum mechanics to it in a usual way[56]. The mentioned environment can be regarded as a discrete set of degrees of freedom, or a set of harmonic oscillators[57]. In addition, the surrounding environment can be modeled as a set of continuum harmonic oscillators[58]. The Hamiltonian describing this model of dissipation is called the Gardiner-Collett Hamiltonian[59]. Also, based on the dissipation of the atomic upper level, a model describing

dissipative atom-field system is introduced[60]. This model described by a non-Hermitian Hamiltonian is called damping JCM. The authors have studied decaying behaviour of the entanglement between atom and field. Also, one of the interesting topics in dissipative systems is to find a way to fight against the decay of the entanglement. Many schemes have been proposed in order to preserve entanglement in such systems. For instance, it has been shown that, the addition of a laser field leads to high stationary entanglement[57]. Another approach to overcome this problem, relies on active feedback[61–63]. In addition to these, the quantum Zeno effect is a promising way to avoid the decaying behaviour of the entanglement in dissipative systems[64–68]. In the dissipation regime, we use the damping deformed JCM to describe a two-level atom interaction with the dissipative cavity and investigate individually and simultaneously the effects of dissipation and detuning parameters on the entanglement between the two-level atom and the deformed field. It has been shown that by detuning modulation, and setting the deformation parameter, coupling constant and average photon number of the field, the degree of entanglement of the atom-field states, and the atomic population inversion may be controlled.

Parity Deformed JCM and Interpretation

The system we introduce here is a parity extension of the standard Jaynes-Cummings model in the rotating-wave approximation, as follows

$$H_\lambda := \frac{\omega}{2}\{\mathfrak{a}, \mathfrak{a}^\dagger\} + \frac{\omega_0}{2}\sigma_3 + g\,(\mathfrak{a}^\dagger\sigma_- + \mathfrak{a}\sigma_+), \tag{12}$$

along with substitution Eqs (8) and (9) in Eq. (12), we can recast the Hamiltonian H_λ into

$$H_\lambda = \frac{\omega}{2}\{a, a^\dagger\} + \frac{\omega}{2}\frac{\lambda(\lambda-1)}{x^2} + \frac{\omega_0}{2}\sigma_3 + g\,(a^\dagger\sigma_- + a\sigma_+) - i\frac{\sqrt{2}g\lambda}{x}\hat{R}\sigma_y, \tag{13}$$

$$= H_{JCM} + \frac{\omega}{2}\frac{\lambda(\lambda-1)}{x^2} - i\frac{\sqrt{2}g\lambda}{x}\hat{R}\sigma_y. \tag{14}$$

It recalls a system of a two-level atom coupled simultaneously to a single-mode of the quantized electromagnetic field and a centrifugally external classical field. It reduces to an ordinary JCM, while $\lambda \to 0$. Here, $\sigma_\pm$ and σ_3 are usual rising (lowering) and inversion operators for the atomic states, $|\pm\rangle$, satisfying $[\sigma+, \sigma_-] = \sigma_3$ and $[\sigma_3, \sigma\pm] = \pm 2\sigma_\pm$, $a^\dagger$ and a are the creation and annihilation operators for the cavity mode $[a, a^\dagger] = 1$, g is the coupling constant between the atom and the cavity field mode, ω and ω_0 are the cavity as well as the external mode frequency and the atomic transition frequency, respectively, λ represents the strength of the external field, $E_{ext}d \equiv \frac{\sqrt{2}g\lambda}{x}\hat{R}$ is the coupling constant between the atom and the external classical field where d recalls the atomic dipole matrix element for the transition and E_{ext} refers to the amplitude of the external field. It is noteworthy that the Hamiltonian H_λ is super-symmetric when $\omega = \omega_0$ (exact resonance) and $g = 0$ (absence of coupling). This exactly solvable model includes the inversely quadratic potential, $\frac{1}{2}\frac{\lambda(\lambda-1)}{x^2}$, first proposed by Post in 1956 when he studied the one-dimensional many identical particles problem in the case of the pair-force interaction between the particles[69]. In addition to the two typical model potentials such as the Morse potential and Poschl-Teller potential, this an-harmonic oscillator potential can be considered as a good candidate to describe the molecular vibrations too[70–72]. Since 1956, this quantum system was studied by other researchers, extensively. For example, Landau and Lifshitz studied its exact solutions in three dimensions[73]. Recently, Sage has studied the vibrations and rotations of the pseudo-gaussian oscillator in order to describe the diatomic molecule[74], in which he briefly reinvestigated some properties of the PHO in order to study the pseudo-gaussian oscillator. Advantages of the pseudo-harmonic potential have been considered for improvements in the conventional presentation of molecular vibrations[75]. Hurley found that this kind of PHO interaction between the particles can be exactly solved by the separation of variables while studying the three-body problem in one dimension[76]. A few years later, Calogero studied the one-dimensional three- and N-body problems interacting pairwise via harmonic and inverse square (centrifugal) potential[77,78]. On the other hand, this potential was generalized by Camiz and Dodonov *et al.* to the non-stationary (varying frequency) PHO potential[79,80]. In addition, such a physical problem was also studied in arbitrary dimension. Also, Dong *et al.* have studied its dynamical group in two dimensions[81].

This parity deformed JCM model possesses an exact solution because of the existence of an integral of motion, $\mathfrak{a}^\dagger\mathfrak{a} + \frac{1}{2}\sigma_3$, which commutes with the Hamiltonian H_λ and allows us to decompose all the representation space of the atom-field system as the tensor product of the Hilbert space associated with the field, $\mathcal{H}_\lambda$, times the Hilbert space associated with the spin, $\mathcal{H}_f$,

$$\mathcal{H} := \mathcal{H}_\lambda \otimes \mathcal{H}_f = \left\{|2n, +\rangle = \begin{pmatrix}|2n\rangle\\0\end{pmatrix}, |2n+1, -\rangle = \begin{pmatrix}0\\|2n+1\rangle\end{pmatrix}\right\}_{n=0}^{\infty}, \tag{15}$$

or

$$\left\{|2n+1, +\rangle = \begin{pmatrix}|2n+1\rangle\\0\end{pmatrix}, |2n+2, -\rangle = \begin{pmatrix}0\\|2n+2\rangle\end{pmatrix}\right\}_{n=0}^{\infty}. \tag{16}$$

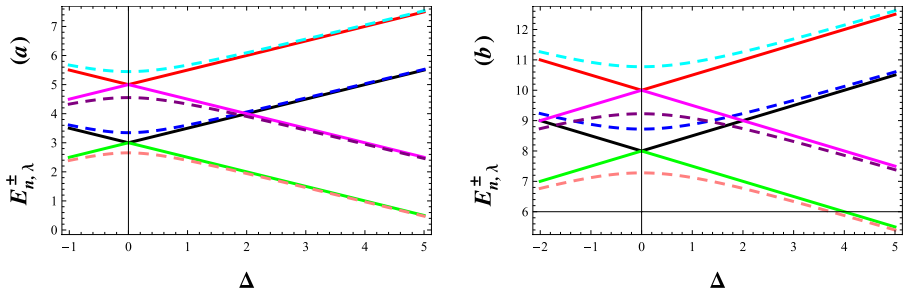

Figure 1. Dependence of eigenvalues $E^{\pm}_{n,\lambda}$ on detuning Δ. The continuous curve corresponds to $g=0.01$. The dashed curves (**a**) and (**b**) correspond to ($g=0$, $\lambda=0$) and ($g=0$, $\lambda=50$), respectively. The dashed curves with positive and negative slopes correspond respectively to $E^{+}_{n,\lambda}$ and $E^{-}_{n,\lambda}$. Lower part of the figure is for $n=1$ and upper part for $n=2$.

Here, $|2n, +\rangle$ is the bare state in which the atom is in the excited state $|+\rangle$ and the field has $2n$ photons, and a similar description holds for the bare state $|2n+1, -\rangle$, where $|-\rangle$ is the atom ground state. Using the Fock space $\mathcal{H}$ given in (15), we can find the following matrix representation of the $\lambda-$deformed JC Hamiltonian H_λ:

$$H_\lambda = \begin{pmatrix} \omega\left(2n+\lambda+\frac{1}{2}\right)+\frac{\omega_0}{2} & g\sqrt{2n+2\lambda+1} \\ g\sqrt{2n+2\lambda+1} & \omega\left(2n+\lambda+\frac{3}{2}\right)-\frac{\omega_0}{2} \end{pmatrix}. \tag{17}$$

It is easy to see that the corresponding dressed eigen-states of H_λ are

$$|E_n^+\rangle = c_1|2n, +\rangle + c_2|2n+1, -\rangle, \tag{18}$$

$$|E_n^-\rangle = c_2|2n, +\rangle - c_1|2n+1, -\rangle, \tag{19}$$

where the coefficients $c_{1(2)}$ are given by:

$$c_1 = \frac{\Delta - \Omega_{n,\lambda}}{\sqrt{\Delta^2 + 4g^2(2n+2\lambda+1)}}, \tag{20}$$

$$c_2 = \frac{2g\sqrt{2n+2\lambda+1}}{\sqrt{(\Delta-\Omega_{n,\lambda})^2 + 4g^2(2n+2\lambda+1)}}, \tag{21}$$

in which $\Delta(=\omega-\omega_0)$ and $\Omega_{n,\lambda}(=\sqrt{\Delta^2+4g^2(2n+2\lambda+1)})$ are defined as detuning parameter and a generalized Rabi frequency, respectively. The energy eigenvalues corresponding to the eigen-states in Eqs (18) and (19) are

$$E^{\pm}_{n,\lambda} = (2n+\lambda+1)\omega \pm \frac{\Omega_\lambda}{2}. \tag{22}$$

The energy difference between the levels $E^{+}_{n,\lambda}$ and $E^{-}_{n,\lambda}$ is $\Omega_{n,\lambda}$. The minimum of the separation occurs when Δ equals to zero and the corresponding difference is $2g\sqrt{2n+2\lambda+1}$. In Fig. 1(a) and (b), respectively, we have plotted the energy eigenvalues $E^{+}_{n,\lambda}$ and $E^{-}_{n,\lambda}$ as functions of Δ for given values of $\lambda=0, 50$. The dotted lines represent the eigenvalues when $g=0$, i.e. $E^{\pm}_{n,\lambda} = (2n+\lambda+1)\omega \pm \frac{\Delta}{2}$. In this case, the eigenvalues cross each other as they increase from negative to positive values. The continuous lines represent the energy eigenvalues for $g=0.01$. The diverging eigenvalue separation beyond the minimum separation indicates level repulsion in the eigenvalues of the dressed states. As Fig. 1(a) and (b) show, the repulsion between energy levels increases as the deformation parameter λ gets bigger. The latter, also, leads to shift the energy levels to the positive side.

Evolution of Atom-Field State

In order to study the influence of the deformation on the dynamics of the parity-deformed JCM, firstly we decompose the Hamiltonian (12) as follows:

$$H_\lambda = H_0 + H', \tag{23}$$

where

$$H_0 = \omega\left(\mathfrak{a}^\dagger\mathfrak{a} + \frac{1}{2} + \lambda\hat{R}\right) + \frac{1}{2}\omega_0\sigma_3, \tag{24}$$

$$H' = g(\mathfrak{a}^\dagger\sigma_- + \mathfrak{a}\sigma_+). \tag{25}$$

In the interaction picture generated by H_0, the Hamiltonian of the system can be written as

$$H_I = e^{iH_0t}H'e^{iH_0t} = g(\mathfrak{a}^\dagger\sigma_- e^{i\Delta t} + \mathfrak{a}\sigma_+ e^{-i\Delta t}). \tag{26}$$

We now proceed to solve the equation of motion of this system in an interaction picture, that is

$$H_I\Psi(t) = i\frac{\partial}{\partial t}\Psi(t). \tag{27}$$

At any time t, the wave function $\Psi(t)$ is expanded in terms of the states $|2n, +\rangle$ and $|2n+1, -\rangle$ as follows

$$\Psi(t) = \sum_{n=0}^{\infty}[c_{+,2n}(t)|2n, +\rangle + c_{-,2n+1}(t)|2n+1, -\rangle] \tag{28}$$

Clearly, $\Psi(t)$ is determined completely once the coefficients $c_{+,2n}(t)$ and $c_{-,2n+1}(t)$ are known. Inserting (28) into (27), we obtain the following general solution for the probability amplitudes, $c_{+,2n}(t)$ and $c_{-,2n+1}(t)$, as:

$$\begin{aligned} c_{+,2n}(t) &= \left\{c_{+,2n}(0)\left[\cos\left(\frac{\Omega_{n,\lambda}}{2}t\right) + i\frac{\Delta}{\Omega_{n,\lambda}}\sin\left(\frac{\Omega_{n,\lambda}}{2}t\right)\right]\right. \\ &\quad \left. - 2ig\frac{\sqrt{2n+2\lambda+1}}{\Omega_{n,\lambda}}c_{-,2n+1}(0)\sin\left(\frac{\Omega_{n,\lambda}}{2}t\right)\right\}e^{-i\frac{\Delta}{2}t}, \end{aligned} \tag{29}$$

$$\begin{aligned} c_{-,2n+1}(t) &= \left\{c_{-,2n+1}(0)\left[\cos\left(\frac{\Omega_{n,\lambda}}{2}t\right) - i\frac{\Delta}{\Omega_{n,\lambda}}\sin\left(\frac{\Omega_{n,\lambda}}{2}t\right)\right]\right. \\ &\quad \left. - 2ig\frac{\sqrt{2n+2\lambda+1}}{\Omega_{n,\lambda}}c_{+,2n}(0)\sin\left(\frac{\Omega_{n,\lambda}}{2}t\right)\right\}e^{i\frac{\Delta}{2}t}, \end{aligned} \tag{30}$$

where the constants $c_{-,2n+1}(0)$ and $c_{+,2n}(0)$ are determined from the initial conditions of the system, which is supposed initially in the upper level, i.e. $c_{+,2n}(0) = c_{2n}(0)$ and $c_{-,2n+1}(0) = 0$. Here, the initial condition for the field is described by $c_{2n}(0)$. For this case in particular, we have

$$c_{+,2n}(t) = c_{2n}(0)\left[\cos\left(\frac{\Omega_{n,\lambda}}{2}t\right) + i\frac{\Delta}{\Omega_{n,\lambda}}\sin\left(\frac{\Omega_{n,\lambda}}{2}t\right)\right]e^{-i\frac{\Delta}{2}t}, \tag{31}$$

$$c_{-,2n+1}(t) = -2ig\frac{\sqrt{2n+2\lambda+1}}{\Omega_{n,\lambda}}c_{2n}(0)\sin\left(\frac{\Omega_{n,\lambda}}{2}t\right)e^{i\frac{\Delta}{2}t}, \tag{32}$$

This set of equations gives us the solution for the problem. In order to calculate some physical quantities of interest, we need only to specify the initial photon number distribution of the field $|c_{2n}(0)|^2$.

The field we are considering in this work is being treated as an λ-deformed oscillator which could be described in different ways. We focus on the situations in which the field as an eigen-state of the λ-deformed annihilation operator is introduced[48], i.e. $\mathfrak{a}^2|W\rangle_{\lambda,+} = w^2|W\rangle_{\lambda,+}$, and its number state expansion is

$$|w\rangle_{\lambda,+} := \sqrt{\frac{\left(\frac{|w|}{\sqrt{2}}\right)^{2\lambda-1}}{I_{\lambda-\frac{1}{2}}(|w|^2)}}\sum_{n=0}^{\infty}\frac{w^{2n}}{\sqrt{2^{2n}n!\Gamma(n+\lambda+\frac{1}{2})}}|2n\rangle. \tag{33}$$

Therefore, in this case, we have

$$|c_{2n}(0)|^2 = \frac{\left(\frac{|w|}{\sqrt{2}}\right)^{4n+2\lambda-1}}{n!\Gamma(n+\lambda+\frac{1}{2})I_{\lambda-\frac{1}{2}}(|w|^2)}. \tag{34}$$

It needs to be noted that, as a second option, one may choose the initial state of the field as the Wigner negative binomial states already studied[49]. They are mathematically equivalent to those nonlinear ones and may be expected to bring new quantum features.

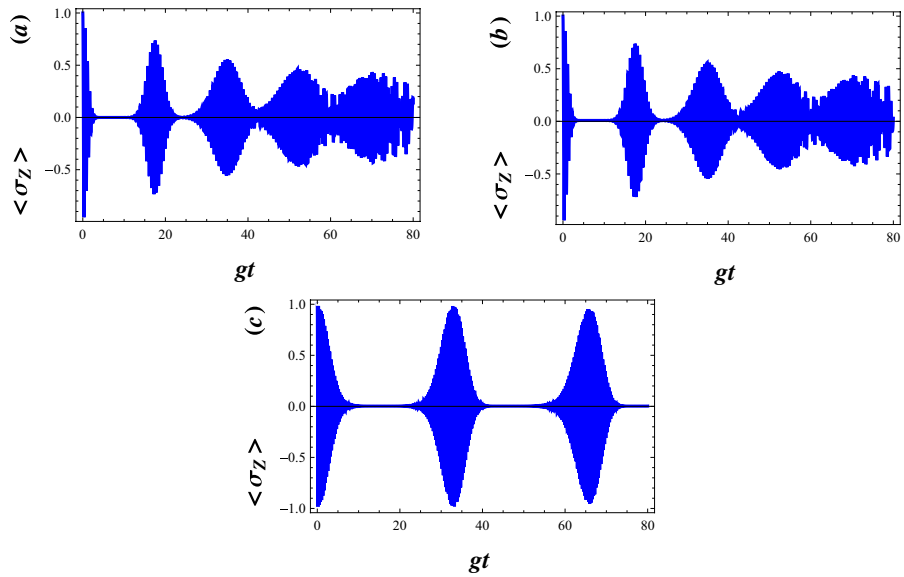

Figure 2. Temporal evolution of the atomic inversion ⟨σz⟩ for the field initially prepared in WCS, $|w\rangle_{\lambda,+}$, with $|w|^2 = 30$ and $g = 0.01$. The parameters are (**a**) $\lambda = 0$, $\Delta = 0$, (**b**) $\lambda = 0$, $\Delta = 0.01$ and (**c**) $\lambda = 50$, $\Delta = 0.01$.

Atomic Dynamics and Dissipative Limit

In this section, we are interested in studying the temporal evolution of atomic inversion, which, in turn, is specified by the expectation value of the inversion operator as:

$$\langle \sigma_z \rangle = \sum_{n=0}^{\infty} (|c_{+,2n}(t)|^2 - |c_{-,2n+1}(t)|^2). \tag{35}$$

Substituting Eqs (31), (32) and (34) into (35), we obtain, for an atom prepared initially in the excited state,

$$\langle \sigma_z \rangle = \sum_{n=0}^{\infty} |c_{2n}(0)|^2 \left[\left(\frac{\Delta}{\Omega_\lambda} \right)^2 + (8n + 8\lambda + 4) \left(\frac{g}{\Omega_\lambda} \right)^2 \cos(\Omega_\lambda t) \right]. \tag{36}$$

The numerical results of the atomic inversion when the field is in a standard cat state (i.e. when $\lambda = 0$), have been shown against the scaled time gt in Fig. 2(a) and (b), respectively. The temporal evolution of the atomic inversion $\langle \sigma_z \rangle$ reveals significant discrepancies of the well-known phenomenon of collapses and revivals[82]. Note that the collapse, i.e. when the envelope of the oscillations collapses to zero, is due to the destructive interference among the probability amplitudes at different Rabi frequencies, $\Omega_{n,\lambda}$, for different photon number eigen-states. At the revival times, on the other hand, constructive interference occurs. This phenomenon also takes place when the initial field state is a WCS. In Fig. 2(c), we have pictured the function $\langle \sigma_z \rangle$ for the value $\lambda = 50$. In this case, $\langle \sigma_z \rangle$ exhibits quasi periodic behaviour very similar to the atomic inversion of a two-photon JCM[83–85], with an effective Hamiltonian defined as $H_{eff} = \omega\left(a^\dagger a + \frac{1}{2}\right) + \frac{\omega_0}{2}\sigma_3 + g(a^{\dagger\,2}\sigma_- + a^2\sigma_+)$. However, in this case, note how the structure of the oscillations is much more complex than the standard Rabi oscillations. As the detuning factor Δ increases, these structures are disappeared (see Fig. 3), i.e. the inhibition of the radiation decay is more transparent. It is clear that the inhibited decay even occurs in the case $\lambda = 0$. This behaviour is due to the influence of the parity deformation via the generalized Rabi frequency $\Omega_{n,\lambda}$. Figure 3(a–c) indicate that, with increasing λ the inhibition decay of the excited state will be balanced.

The finite lifetime of the atomic levels can be described by adding phenomenological decay terms, $-i\frac{\gamma}{2}|+\rangle\langle+|$, to the Hamiltonian (9), where $\gamma \in \mathbb{R}$ is a decay constant[60]. For an atom initially stated in the upper level, $|+\rangle$, the population inversion dynamics are analyzed for a deformed JCM was surrounded by a dissipative environment where the dissipation of the upper-level is considered (see Fig. 4). Here, we plot the dynamics of the population inversion in the presence of the decay term against the scaled time gt. In Fig. 4, we compare the effects of increasing γ on the Rabi oscillations, where the latter is destroyed. However, as is illustrated in Fig. 5, the patterns of the revivals are restored while λ is enhanced.

Fidelity

We now calculate the fidelity

$$F = |\langle \Psi(0)|\Psi(t)\rangle|^2, \tag{37}$$

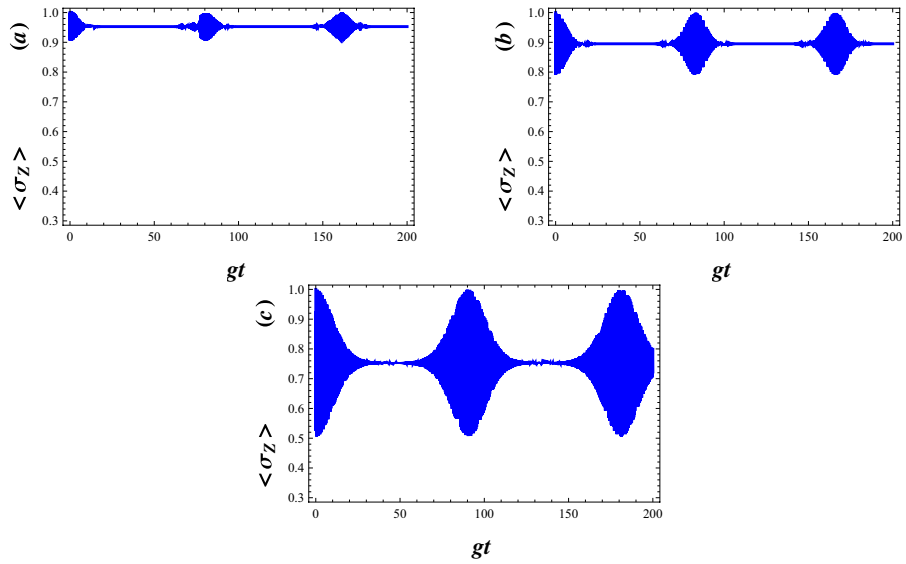

Figure 3. Temporal evolution of the atomic inversion with $|w|^2 = 30$, $g = 0.01$ and $\Delta = 0.5$. The parameters equal to (**a**) $\lambda = 0$, (**b**) $\lambda = 30$ and (**c**) $\lambda = 100$.

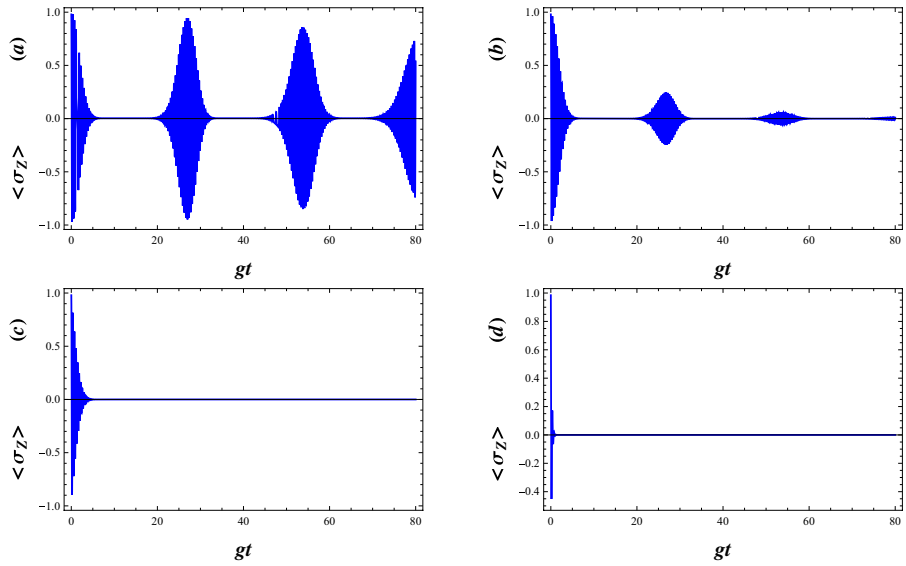

Figure 4. Temporal evolution of the atomic inversion with $|w|^2 = 30$, $g = 0.01$, $\Delta = 0.5$ and $\lambda = 30$. The parameters equal to (**a**) $\gamma = 0$, (**b**) $\gamma = 0.001$, (**c**) $\gamma = 0.01$ and $\gamma = 0.1$.

which measures the "closeness" of the two quantum states $|\Psi(t)\rangle$ and $|\Psi(0)\rangle = |w\rangle_{\lambda,+} \otimes |+\rangle$, which indicate that F is unity when these two quantum states are identical. Figure 6 indicates that with increasing λ the fidelity decreases but remains close to its initial value (see Fig. 5(a)–(d)). To obtain fidelity around 1, one needs to enhance the deformation parameter λ to 100 and $gt = 95$. In this case, $|\Psi(t)\rangle$ becomes minimum uncertainty state which minimize the uncertainty relation, Eq. (28) in ref. 48.

Generation of Maximally Entangled States

Entanglement is a striking feature of the quantum mechanics can be compared with the classical ones[86]. This phenomenon as a nonlocal correlation between two (or more) quantum systems plays a fundamental role in the quantum information science such as quantum computation and communication[87–89], teleportation[90], dense coding[91,92], cryptography[93] and etc. Generally, characterization of amount of entanglement is achieved through the well justified and mathematically tractable measures[94]. For bipartite states, a number of acceptable entanglement measures such as the entanglement of formation and distillation[95], concurrence, negativity[96], Von Neumann entropy and relative entropy[97] have been proposed. In this section, in order to obtain the degree of entanglement between atom and field, we choose the Von Neumann entropy. The Von Neumann entropy is a very useful

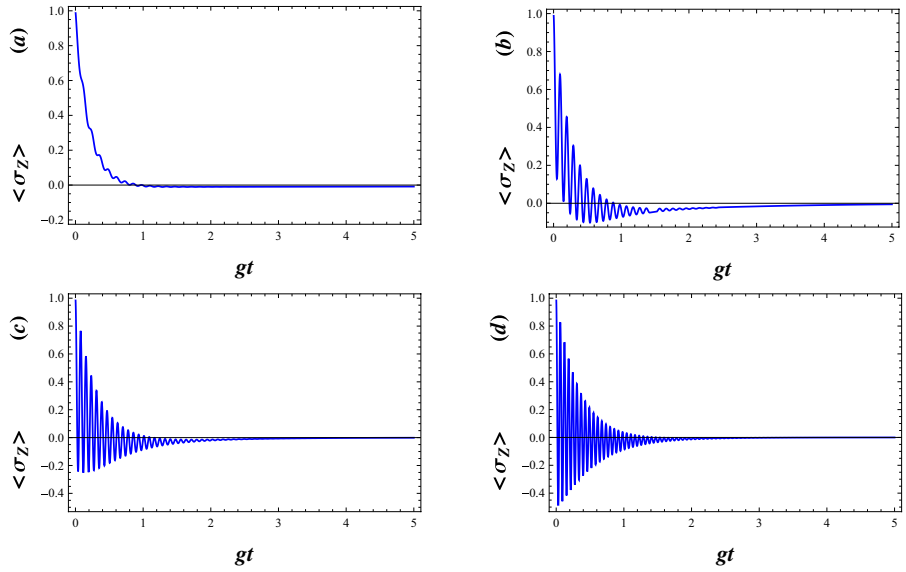

Figure 5. Temporal evolution of the atomic inversion with $|w|^2 = 30$, $g = 0.01$, $\Delta = 0.5$ and $\gamma = 0.05$. The parameters equal to (**a**) $\lambda = 0$, (**b**) $\lambda = 200$, (**c**) $\lambda = 500$ and $\lambda = 1000$.

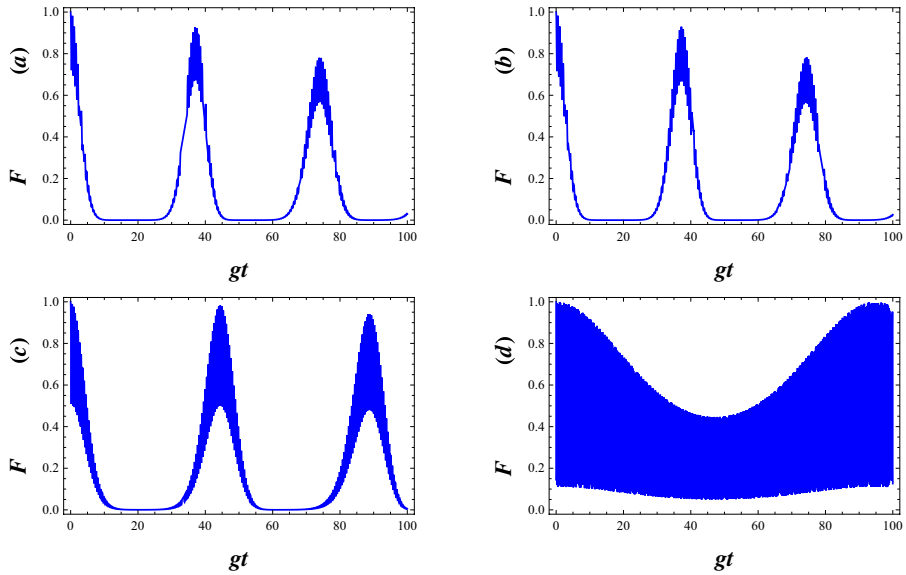

Figure 6. Fidelity as a function of the scaled time of gt in the small coupling regime with $g = 0.01$ for different $\lambda(= -0.25, 0, 10, 100)$, other parameters are $|w|^2 = 9$ and $\Delta = 0.1$.

operational measure of the disorder of a system and of the purity of a quantum state. For given density operator ρ the Von Neumann entropy is given by

$$S(\rho) := \mathrm{Tr}[\rho \ \ln \ \rho], \tag{38}$$

where "Tr" often abbreviated to the trace and $S(\rho)$ ranges from 0 for a separable state to 1 for a maximally entangled one. As the deformed JCM is a bipartite system, a Schmidt decomposition is assured. Based on the solution of the time-dependent Schrodinger equation (23), and according to the Schmidt decomposition, for any instant in time t, we can always find the reduced density operator of the atom in the bare basis specified by $|\pm\rangle$ and obtain

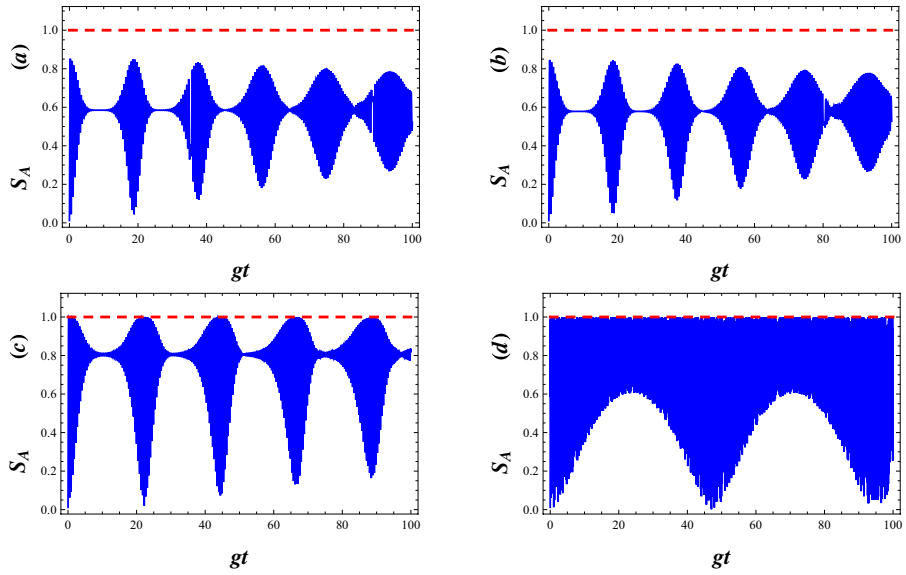

Figure 7. Plots of entropy S_A versus gt with $g=0.01$, $|w|^2=9$ and $\Delta=0.1$ for various deformation parameters respectively (**a**) $\lambda=-0.25$, (**b**) $\lambda=0$, (**c**) $\lambda=10$ and (**d**) $\lambda=50$.

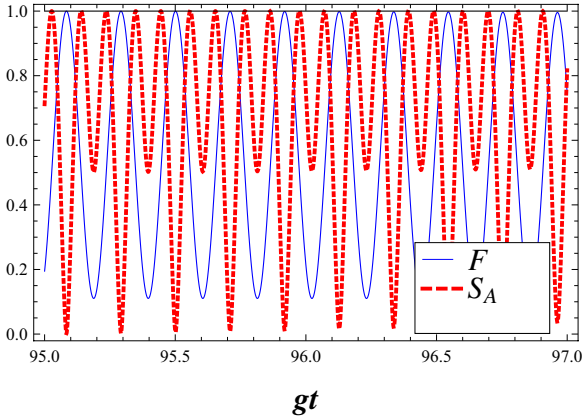

Figure 8. The Von Neumann entropy (dash) and the fidelity (solid) are plotted together. In each case a deformation parameter with $\lambda=100$, $g=0.01$, $|w|^2=9$, $\Delta=0.1$ is used.

$$\rho_A = \begin{pmatrix} \sum_{n=0}^{\infty} |c_{+,2n}(t)|^2 & 0 \\ 0 & \sum_{n=0}^{\infty} |c_{-,2n+1}(t)|^2 \end{pmatrix}. \tag{39}$$

Clearly, eigenvalues of the density operator for the atom, $g_{\pm}$, can be expressed in terms of the coefficients $c_{+,2n}(t)$ and $c_{-,2n+1}(t)$ i.e. $g_+ = \sum_{n=0}^{\infty} |c_{+,2n}(t)|^2$ and $g_- = \sum_{n=0}^{\infty} |c_{-,2n+1}(t)|^2$. Then, it is easy to obtain an expression for the Von Neumann entropy. For atomic subsystem, this is:

$$S_A = -g_+ \ln g_+ - g_- \ln g_-. \tag{40}$$

In Fig. 7, for an atom initially in an excited state and the field initially in WCS, we plot the Von Neumann entropy S_A, all against the scaled time gt. We can also see that the entropy makes quasi-period oscillation. This means that the deformed field can help to realize and stabilize the degree of entanglement between the atom and the field at a high level. Sometimes, as the deformation parameter λ is enhanced, the atom- field system becomes maximally entangled (Fig. 7(c) and (d)). In Fig. 8, we compare the Von Neumann entropy and fidelity of the quantum state, $\Psi(t)$, associated with the $\lambda-$deformed JCM investigated here. Bear in mind that entanglement between the atom and field is maximized i.e. the quantum state $\Psi(t)$ becomes maximally entangled, where fidelity of the quantum state passes the smallest value.

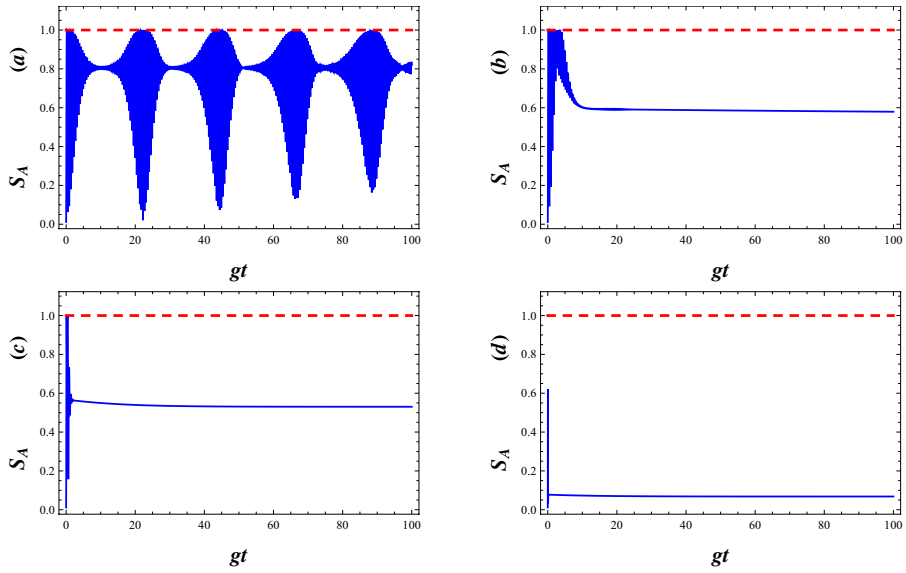

Figure 9. The time evolution of atomic entropy S_A in the dissipative regime for $g=0.01$, $|w|^2=9$, $\Delta=0.1$ and $\lambda=2$, (**a**) $\gamma=0$, (**b**) $\gamma=0.01$, (**c**) $\gamma=0.1$ and (**d**) $\gamma=1$.

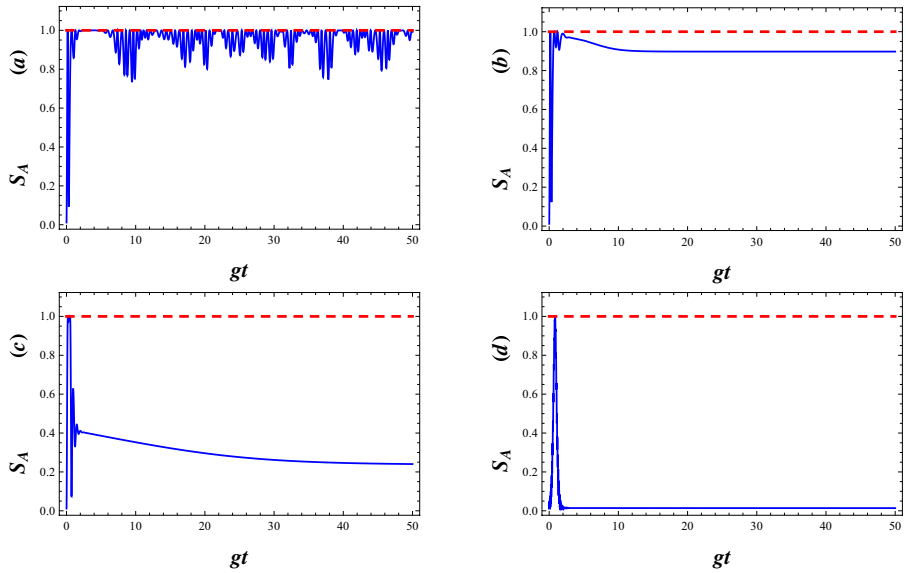

Figure 10. The time evolution of atomic entropy S_A in the dissipative regime with $g=0.01$, $|w|^2=9$, $\lambda=2$ and $\gamma=0.1$, (**a**) $\Delta=0$, (**b**) $\Delta=0.01$, (**c**) $\Delta=0.1$ and (**d**) $\Delta=1$.

Dissipative Regime and Robust Entangled states

Now, we consider the dynamics of entanglement between atom and field in dissipative regime. For this purpose, the time evolution of the Von Neumann entropy for different decay coefficients near the resonant case has been plotted in Fig. 9. In an ideal case which no decay rate is considered, as is shown in Fig. 9(a), S_A suddenly increases from 0 to its maximum value and then the collapse and revival patterns around the 0.8 (a amount near its maximum value) are presented. In the actual system, the atom is steady when it is in the ground state. However, when the atom is in the excited state, some factors such as the spontaneous emission, the collision between atoms and so on, will lead to the decay of the upper-level. In this case, S_A attains a stable behaviour after some fluctuations at the beginning of the interaction (see Fig. 9(b–d)). As is seen, the increment of the decay coefficients not only disappears the rapidly oscillations of S_A in the initial times, but also leads to a reduction of the amount of entanglement.

In Fig. 10, to investigate the influence of the field frequency modulation on the atom-field entanglement, we set different modulation frequencies. When we compare Fig. 10 with Fig. 9, we find that the entanglement can last a longer time as Δ decreases. The entanglement decays to zero in the larger detuning parameter while the entanglement still exists in the resonant case. However, the maximum of the entropy decreases with an increase in Δ (see Fig. 10(b)). The small detuning, $\Delta<1$, reduces the maximum value of entanglement in the short time region,

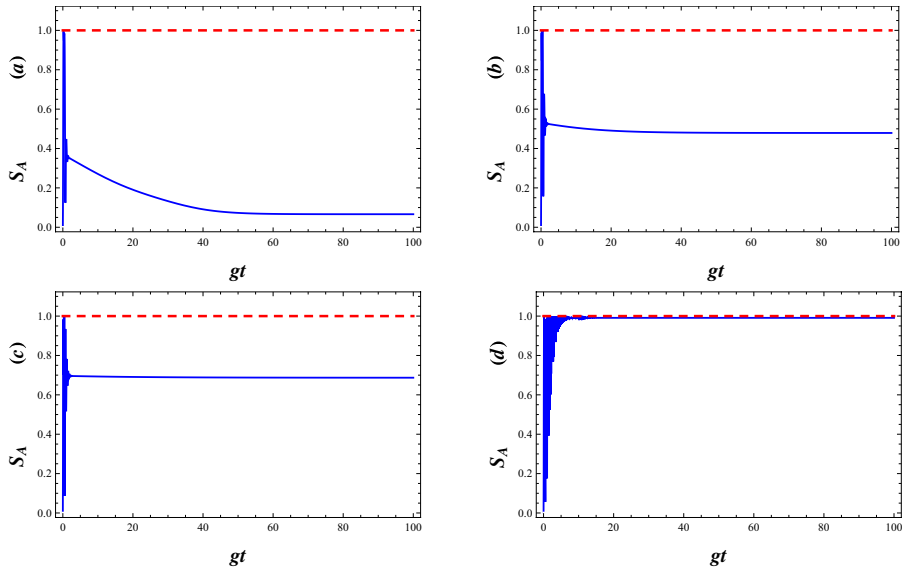

Figure 11. The time evolution of atomic entropy S_A in the dissipative regime with $g=0.01$, $|w|^2=9$, $\gamma=0.1$ and $\Delta=0.1$, (**a**) $\lambda=0$, (**b**) $\lambda=10$, (**c**) $\lambda=20$ and (**d**) $\lambda=80$.

while it prolongs the entanglement time. Comparison of Fig. 10(b) with Fig. 10(d), reveals that larger modulation is unfavorable to the maintenance of the entanglement for a long time.

Fig. 11 refers to the effect of the parity deformation on time evolution of the entanglement. As is shown, in the absence of λ, the atomic entropy after suddenly increasing to its maximum value at the beginning of the interaction, decay to a minimum asymptotic (stable) value in enough large times (see Fig. 11(a)). As is seen, the presence of λ not only decreases the decay time but also causes the enhancement of the asymptotic (stable) values of atomic entropy (see Fig. 11(c–d)) in which for large values of λ, the stable values of entanglement reaches to 1. On the other words, by increasing λ the generated maximally entangled states are preserved, in the dissipation regime at the beginning of the interaction.

Non-classical Properties: Sub-Poisonian Statistics and Squeezing Effect

We now examine the time evolution of the nonclassical properties of the constructed states $\Psi(t)$. To achieve this purpose, we investigate the sub-Poissonian statistics and their quadrature squeezing. It should be mentioned that squeezing or sub-Poissonian statistics are sufficient requirements for a state to belong non-classical ones. The anti-bunching effect as well as the sub-Poissonian statistics of the states $\Psi(t)$ is investigated by evaluating Mandel's Q^λ parameters, which are defined as

$$Q^\lambda = \frac{\langle(\mathfrak{a}^\dagger\mathfrak{a})^2\rangle - \langle\mathfrak{a}^\dagger\mathfrak{a}\rangle^2}{\langle\mathfrak{a}^\dagger\mathfrak{a}\rangle} - 1. \tag{41}$$

The inequality $Q<0$ indicates the sub-Poissonian photon number distribution, which implies that photons are antibunched. It is well know that sub-Poissonian statistics is a signature of the quantum nature of the field. Conversely, $Q>0$ holds for a super-Poissonian photon number distribution. Also, $Q=0$ corresponds to the canonical coherent state. Here, the angular brackets denote averaging any field operator $\hat{O}$ over an arbitrary normalizable state $\Psi(t)$ for which the mean values are well defined, i.e.

$$\begin{aligned}\langle\hat{O}\rangle &= \sum_{n,m}^{\infty}[c^*_{+,2m}(t)c_{+,2n}(t)\langle 2m,+|\hat{O}|2n,+\rangle \\ &+ c^*_{-,2m+1}(t)c_{-,2n+1}(t)\langle 2m+1,-|\hat{O}|2n+1,-\rangle],\end{aligned} \tag{42}$$

where the probability amplitudes $c_{+,2n}$ and $c_{-,2n+1}(t)$ are given by equations (26) and (27), respectively. In Fig. 12, we have shown the temporal evolution of the Mandel's Q^λ parameters given by equation (41), when the field is initially in the WCS. It has been demonstrated that its statistics tend to fluctuate around Poissonian conduct for small values of λ(see Fig. 12(a) and (c)). On the other hand, the statistics of the system exhibits, in general, a super-Poissonian behaviour for the same $|w|^2$ initial value while $\lambda>0$.

Squeezing of radiation is a purely nonclassical phenomenon without any classical analogue and has attracted considerable attention owing to its low-noise property. It has been either experimentally observed or theoretically predicted in a variety of nonlinear optical processes. Now, let us consider the squeezing properties of the field by introducing the following two Hermitian field amplitudes, $\hat{x}\left(=\frac{\mathfrak{a}+\mathfrak{a}^\dagger}{\sqrt{2}}\right)$ and $\hat{p}_\lambda\left(=\frac{\mathfrak{a}-\mathfrak{a}^\dagger}{i\sqrt{2}}\right)$. The uncertainty relation for the variances of these operators are obtained as

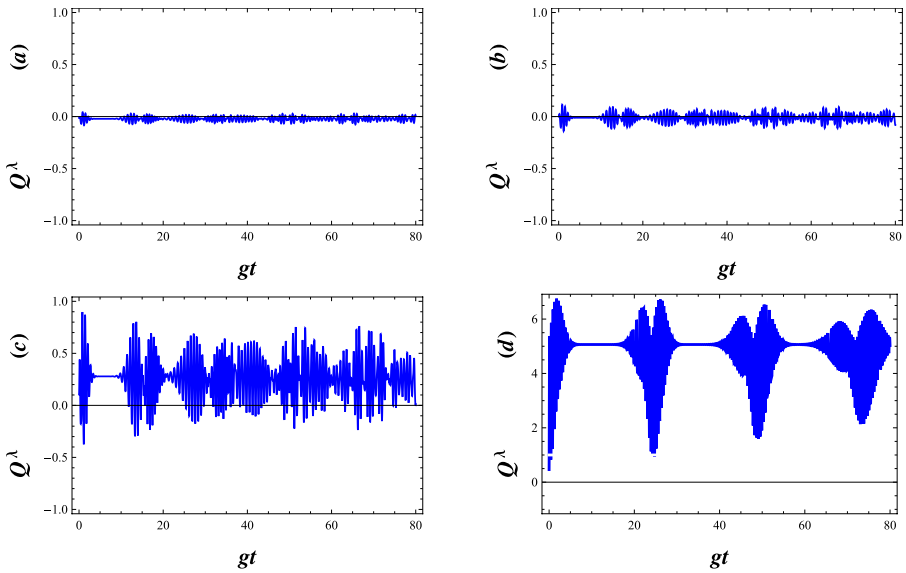

Figure 12. Plots of the normalized variance, Q^λ, as a function of the normalized time gt, for the field initially prepared in an annihilation operator coherent state $|w\rangle_{\lambda,+}$ with $|w|^2 = 20$, $g = 0.01$ and $\Delta = 0.01$. The parameters are (**a**) $\lambda = -0.25$, (**b**) $\lambda = 0$, (**c**) $\lambda = 2$ and (**d**) $\lambda = 10$.

$$\langle \sigma_{xx} \rangle \langle \sigma_{pp} \rangle \geq \frac{\left| \langle 1 + 2\lambda \hat{R} \rangle \right|^2}{4}, \tag{43}$$

where $\langle \sigma_{\hat{x}\hat{y}} \rangle = \frac{\langle \hat{x}\hat{y} + \hat{y}\hat{x} \rangle}{2} - \langle \hat{x} \rangle \langle \hat{y} \rangle$ and the angular brackets denote averaging over an arbitrary normalizable state for which the mean values are well defined, $\langle \hat{y} \rangle = \langle \Psi(t) | \hat{y} | \Psi(t) \rangle$. It can be said that a state is squeezed if the condition $\langle \sigma_{xx} \rangle < \frac{|\langle 1 + 2\lambda \hat{R} \rangle|}{2}$ or $\langle \sigma_{pp} \rangle < \frac{|\langle 1 + 2\lambda \hat{R} \rangle|}{2}$ is fulfilled[98,99]. In other words, a quantum state is called squeezed state if it has less uncertainty, in one parameter ($\hat{x}$ or $\hat{p}$), than a coherent state. Then to measure the degree of squeezing, we introduce the squeezing factors $S_{x(p)}$[100], corresponding with the state $\Psi(t)$, respectively

$$S_x = \frac{\langle \sigma_{xx} \rangle - \frac{|\langle 1 + 2\lambda \hat{R} \rangle|}{2}}{\frac{|\langle 1 + 2\lambda \hat{R} \rangle|}{2}}, \tag{44}$$

$$S_p = \frac{\langle \sigma_{pp} \rangle - \frac{|\langle 1 + 2\lambda \hat{R} \rangle|}{2}}{\frac{|\langle 1 + 2\lambda \hat{R} \rangle|}{2}}, \tag{45}$$

which results that the squeezing condition takes the simple form $S^\lambda_{x(p),i} < 0$. By using the mean values of the generators of the WHA,

$$\langle \mathfrak{a} \rangle = \langle \mathfrak{a}^\dagger \rangle = 0 \tag{46}$$

$$\begin{aligned} \langle \mathfrak{a}^2 \rangle &= \sum_n^\infty [c^*_{+,2n}(t) c_{+,2n+2}(t) \sqrt{(2n+2)(2n+2\lambda+1)} \\ &\quad + c^*_{-,2n+1}(t) c_{-,2n+3}(t) \sqrt{(2n+2)(2n+2\lambda+3)}] \end{aligned} \tag{47}$$

$$\begin{aligned} \langle \mathfrak{a}^{\dagger\,2} \rangle &= \overline{\langle \mathfrak{a}^2 \rangle} \\ \langle \mathfrak{a}^\dagger \mathfrak{a} \rangle &= \sum_n^\infty [(2n) |c_{+,2n}(t)|^2 + (2n + 2\lambda + 1) |c_{-,2n+1}(t)|^2] \end{aligned} \tag{48}$$

$$\langle \mathfrak{a}\mathfrak{a}^\dagger \rangle = \sum_n^\infty [(2n + 2\lambda + 1) |c_{+,2n}(t)|^2 + (2n+2) |c_{-,2n+1}(t)|^2] \tag{49}$$

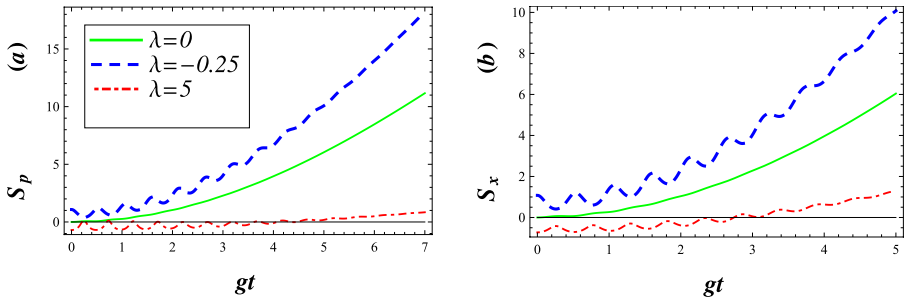

Figure 13. Squeezing in the p and x quadratures against gt for different values of λ with $g = 0.01$, $|w|^2 = 9$ and $\Delta = 0.1$ as well as for fixed values of $\phi = 0$ and $\frac{\pi}{2}$ correspond with (**a**) and (**b**), respectively. The solid curve is plotted for $\lambda = 0$.

$$\langle 1 + 2\lambda\hat{R}\rangle = \sum_{n}^{\infty}[(1 + 2\lambda)|c_{+,2n}(t)|^2 + (1 - 2\lambda)|c_{-,2n+1}(t)|^2] \tag{50}$$

one can derive the variance and covariance of the operators $\hat{x}$ and $\hat{p}$. From Eqs (44) and (45), we also stress that the squeezing is very sensitive to the deformation parameter λ, which can be discussed as follows

- Figure 13(a) and (b) visualize variations of the squeezing factors S_p and S_x in terms of gt for different values of the deformed parameter $\lambda = -0.25$, 0 and 5 when we choose the phase $\phi = 0$ and $\frac{\pi}{2}$, respectively. These show that the squeezing effect in the field operator p may be considerable for $\phi = 0$ and small values of gt while $\lambda > 0$. As seen in Fig. 13(a), the squeezing factor S_p tends to zero which indicates that the states $\Psi(t)$ become minimum uncertainty ones.
- For the case $\phi = 0$, our calculations show that the squeezing factors S_p are really dependent on λ. Figure 13(a) shows that, with a rise in λ, the degree of squeezing or depth of non-classicality increases at first and then decreases when time goes on.
- Squeezing in the p quadrature disappears when ϕ reaches $\frac{\pi}{2}$, where squeezing in the x quadrature is raised (see Fig. 13(b)).

Conclusions

A parity deformed Jaynes-Cummings Hamiltonian in terms of spin and λ-deformed bosonic operators, was introduced. Its eigen-states and eigenvalues were obtained explicitly. Mathematical and physical implications and applications of our results were discussed in detail. The deformed JCM introduced here may add new insights to nonclassical states of radiation in cavity QED. It, also, can be used to further investigate the interaction between an atomic system and a single mode of an electromagnetic field, including damping or amplifying processes, which are of fundamental importance, in quantum optics. By assuming that the atom is initially prepared in the excited state and the field is in the WCS, its quantum dynamical features such atomic inversion, quantum statistics and squeezing of obtained wave functions of the system were investigated. It was found that the atomic inversion exhibits Rabi oscillations including quasi-periodic behavior. Further examination of non-classical signs of the atom-field states, revealed that a significant squeezing can be achieved for positive deformation parameters. Furthermore, increasing the deformation parameter (the stronger external field) changes their statistics from the Poissonian to super-Poissonian. The λ- deformed JCM, driven JCM, can be applied to generate maximally entangled states. In other words, the small detuning and coupling regimes with a large deformation parameter may lead to a long-lasting robust maximally entangled quantum state. It was illustrated that for large values of λ, the generated maximally entangled quantum state was preserved as time goes on, despite the presence of the dissipation. It is worth mentioning that the approach presented here can be potentially compared with some others, already discussed in the literature, where other researchers tried to generate and stabilize the entanglement. In other words, we investigate how an appropriate choice of the external field allows one to control atom-field entanglement. Finally, a possible generalization to the three-level system can be discussed.

References

1. Jaynes, E. & Cummings, F. Comparison of quantum and semiclassical radiation theories with application to the beam maser. *Proc. IEEE* **51,** 89 (1963).
2. Narozhny, N. B., Sanchez-Mondragon, J. J. & Eberly, J. H. Coherence versus incoherence: Collapse and revival in a simple quantum model. *Phys. Rev. A* **23,** 236 (1981).
3. Agarwal, G. S. Vacuum-Field Rabi Splittings in Microwave Absorption by Rydberg Atoms in a Cavity. *Phys. Rev. Lett.* **53,** 1732 (1984).
4. Cummings, F. W. Stimulated Emission of Radiation in a Single Mode. *Phys. Rev* **140,** A 1051 (1965).
5. Phoenix, S. J. D. & Knight, P. L. Fluctuations and entropy in models of quantum optical resonance. *Ann. Phys* **186,** 381 (1988).
6. Chang, D. E., Vuletic, V. & Lukin, M. D. Quantum nonlinear optics — photon by photon. *Nat. Photon* **8,** 685 (2014).
7. Zhang, Y. *et al.* Photon Devil's staircase: Photon long-range repulsive interaction in lattices of coupled resonators with Rydberg atoms. *Sci. Rep* **5,** 11510 (2015).

8. Pedernales, J. S. *et al.* Quantum Rabi Model with Trapped Ions. *Sci. Rep* **5,** 15472 (2015).
9. Zhou, L. & Sheng, Y. B. Complete logic Bell-state analysis assisted with photonic Faraday rotation. *Phys. Rev. A* **92,** 042314 (2015).
10. Forn-Diaz, P., Romero, G., Harmans, C. J. P. M., Solano, E. & Mooij, J. E. Broken selection rule in the quantum Rabi model. *Sci. Rep* **6,** 26720 (2016).
11. Song *et al.* Heralded quantum repeater based on the scattering of photons off single emitters using parametric down-conversion source. *Sci. Rep* **6,** 28744 (2016).
12. Short, R. & Mandel, L. Observation of Sub-Poissonian Photon Statistics. *Phys. Rev. Lett.* **51,** 384 (1983).
13. Lo Franco, R., Compagno, G., Messina, A. & Napoli, A. Bell's inequality violation for entangled generalized Bernoulli states in two spatially separate cavities, *Phys. Rev. A* **72,** 053806 (2005).
14. Lo Franco, R., Compagno, G., Messina, A. & Napoli, A. Single-shot generation and detection of a two-photon generalized binomial state in a cavity. *Phys. Rev. A* **74,** 045803 (2006).
15. Lo Franco, R., Compagno, G., Messina, A. & Napoli, A. Generating and revealing a quantum superposition of electromagnetic-field binomial states in a cavity. *Phys. Rev. A* **76,** 011804(R) (2007).
16. Goy, P., Raimond, J. M., Gross, M. & Haroche, S. Observation of Cavity-Enhanced Single-Atom Spontaneous Emission. *Phys. Rev. Lett.* **50,** 1903 (1983).
17. Singh, S. Field statistics in some generalized Jaynes-Cummings models. *Phys. Rev. A* **25,** 3206 (1982).
18. Tavis, M. & Cummings, F. W. N atoms interacting with a single mode radiation field. *Phys. Rev* **170,** 379 (1968).
19. Sukumar, C. V. & Buck, B. Some soluble models for periodic decay and revival. *J. Phys. A* **17,** 885 (1984).
20. Buzano, C., Rasetti, M. G. & Rastello, M. L. Dynamical Superalgebra of the "Dressed" Jaynes-Cummings Model. *Phys. Rev. Lett* **62,** 137 (1989).
21. Chaichian, M., Ellinas, D. & Kulish, P. Quantum algebra as the dynamical symmetry of the deformed Jaynes-Cummings model. *Phys. Rev. Lett* **65,** 980 (1990).
22. de los Santos-Sanchez, O. & Recamier, J. The *f*-deformed Jaynes–Cummings model and its nonlinear coherent states. *J. Phys. B: At. Mol. Opt. Phys* **45,** 015502 (2012).
23. Aleixo, A. N. F., Balantekin, A. B. & Candido Ribeiro, M. A. A generalized Jaynes-Cummings Hamiltonian and supersymmetric shape invariance. *J. Phys. A: Math. Gen* **33,** 3173 (2000).
24. Wigner, E. Do the Equations of Motion Determine the Quantum Mechanical Commutation Relations?. *Phys. Rev* **77,** 711 (1950).
25. Green, H. S. A Generalized Method of Field Quantization. *Phys. Rev.* **90,** 270 (1953).
26. Volkov, D. V. *On the quantization of half-integer spin fields. Sov. Phys. JETP* **9,** 1107 (1959).
27. Volkov, D. V. *SU(3)×SU(3)* symmetry and the baryon meson coupling constants. *Sov. Phys. JETP* **11,** 375 (1960).
28. Greenberg, O. W. Spin and Unitary Spin Independence in a Paraquark Model of Baryons and Mesons. *Phys. Rev. Lett.* **13,** 598 (1964).
29. Greenberg, O. W. & Messiah. A. M. L. Selection Rules for Parafields and the Absence of Para Particles in Nature. *Phys. Rev. B* **138,** 1155 (1965).
30. Govorkov, A. B. Parastatistics and Parafields. *Theor. Math. Phys* **54,** 234 (1983).
31. Plyushchay, M. S. Deformed Heisenberg algebra with reflection. *Nucl. Phys. B* **491,** 619 (1997).
32. Ohnuki, Y. & Kamefuchi, S. *Quantum Field Theory and Parastatistics. University Press of Tokyo* (1982).
33. Macfarlane, A. J. Generalized Oscillator Systems and Their Parabosonic Interpretation, in Proc. Inter. Workshop on Symmetry Methods in Physics, ed. Sissakian, A. N., Pogosyan, G. S. & Vinitsky, S. I. (JINR, Dubna, 1994).
34. Macfarlane, A. J. Algebraic structure of parabose Fock space. I. The Green's ansatz revisited. *J. Math. Phys* **35,** 1054 (1994).
35. Jayaramants, J. & de Lima Rodrigues, R. The Wigner-Heisenberg algebra as an effective operator technique for simpler spectral resolution of general oscillator-related potentials and the connection with the SUSYQM algebra. *J. Phys. A: Math. Gen* **23,** 3123 (1990).
36. Meljanac, S., Milekovic, M. & Stojic, M. Permutation invariant algebras, a Fock space realization and the Calogero model. *Eur. Phys. J. C* **24,** 331 (2002).
37. Yang, L. M. A Note on the Quantum Rule of the Harmonic Oscillator. *Phys. Rev* **84,** 788 (1951).
38. Polychronakos, A. P. Exchange operator formalism for integrable systems of particles. *Phys. Rev. Lett* **69,** 703 (1992).
39. Brink, L., Hansson, T. H. & Vasiliev, M. A. Explicit solution to the N body Calogero problem. *Phys. Lett. B* **286,** 109 (1992).
40. Brink, L., Hansson, T. H., Konstein, S. & Vasiliev, M. A. The Calogero model: Anyonic representation, fermionic extension and supersymmetry. *Nucl. Phys. B* **401,** 591 (1993).
41. Brzezinski, T., Egusquiza, I. L. & Macfarlane, A. J. Generalized harmonic oscillator systems and their Fock space description. *Phys. Lett. B* **311,** 202 (1993).
42. Plyushchay, M. S. Deformed Heisenberg algebra, fractional spin fields and supersymmetry without fermions. *Ann. Phys.* **245,** 339 (1996).
43. Plyushchay, M. S. Minimal bosonization of supersymmetry. *Mod. Phys. Lett. A* **11,** 397 (1996).
44. Plyushchay, M. S. Deformed Heisenberg algebra and fractional spin field in (2+1)-dimensions. *Phys. Lett. B* **320,** 91 (1994).
45. Aglietti, U., Griguolo, L., Jackiw, R., Pi, S. Y. & Seminara, D. Anyons and Chiral Solitons on a Line. *Phys. Rev. Lett* **77,** 4406 (1997).
46. Horváthy, P. A. & Plyushchay, M. S. Anyon wave equations and the noncommutative plane. *Phys. Lett. B* **595,** 547 (2004).
47. de Matos Filho, R. L. & Vogel, W. Nonlinear coherent states. *Phys. Rev. A* **54,** 4560 (1996).
48. Dehghani, A., Mojaveri, B., Shirin, S. & Saedi, M. Cat-states in the framework of Wigner–Heisenberg algebra. *Ann. Phys* **362,** 659 (2015).
49. Mojaveri, B. & Dehghani, A. Even and odd Wigner negative binomial states: Nonclassical properties. *Mod. Phys. Lett. A* **30,** 1550198 (2015).
50. Bellomo, B., Lo Franco, R. & Compagno, G. Non-Markovian Effects on the Dynamics of Entanglement. *Phys. Rev. Lett* **99,** 160502 (2007).
51. Yu, T. & Eberly, J. H. Quantum Open System Theory: Bipartite Aspects. *Phys. Rev. Lett* **97,** 140403 (2006).
52. Yu, T. & Eberly, J. H. Sudden Death of Entanglement. *Science* **323,** 598 (2009).
53. Mazzola, L., Piilo, J. & Maniscalco, S. Sudden Transition between Classical and Quantum Decoherence. *Phys. Rev. Lett* **104,** 200401 (2010).
54. Bateman, H.On Dissipative Systems and Related Variational Principles. *Phys. Rev* **38,** 815 (1931).
55. Stuckens, C. & Kobe, D. H. Quantization of a particle with a force quadratic in the velocity. *Phys. Rev. A* **34,** 3565 (1986).
56. Dutra, S. M. *Cavity Quantum Electrodynamics: The Strange Theory of Light in a Box*. John Wiley and Sons, New York (2005).
57. Soltani, M. *et al.* Control of entanglement between two dissipative non-interacting qubits in a common heat bath by a laser field. *Eur. Phys. J. D* **67,** 256 (2013).
58. Nourmandipour, A. & Tavassoly, M. K. A novel approach to entanglement dynamics of two two-level atoms interacting with dissipative cavities. *Eur. Phys. J. Plus* **130,** 148 (2015).
59. Collett, M. J. & Gardiner, C. W. Squeezing of intracavity and traveling-wave light fields produced in parametric amplification. *Phys. Rev. A* **30,** 1386 (1984).
60. Scully, M. O. & Zubairy, M. S. *Quantum Optics. Cambridge.* Univ. Press (2001).
61. Sayrin, C. *et al.* Real-time quantum feedback prepares and stabilizes photon number states. *Nature* **477,** 73 (2011).
62. Vijay, R. *et al.* Stabilizing Rabi oscillations in a superconducting qubit using quantum feedback. *Nature* **490,** 77 (2012).

63. Schindler, P. *et al.* Quantum simulation of dynamical maps with trapped ions. *Nat. Phys* **9,** 361 (2013).
64. Misra, B. & Sudarshan, E. C. G. The Zeno's paradox in quantum theory. *J. Math. Phys* **18,** 756 (1977).
65. Koshino, K. K. & Shimizu, A. Quantum Zeno effect by general measurements. *Phys. Rep* **412,** 191 (2005).
66. Facchi, P., Nakazato, H. & Pascazio, S. From the Quantum Zeno to the Inverse Quantum Zeno Effect. *Phys. Rev. Lett.* **86,** 2699 (2001).
67. Facchi, P. *et al.* Control of decoherence: Analysis and comparison of three different strategies. *Phys. Rev. A* **71,** 022302 (2005).
68. Nourmandipour, A. & Tavassoly, M. K. Dynamics and protecting of entanglement in two-level systems interacting with a dissipative cavity: the Gardiner–Collett approach. *J. Phys. B: At. Mol. Opt. Phys* **48,** 165502 (2015).
69. Post, H. R. Many-particles systems: II. Proc. *Phys. Soc. (London). A* **69,** 936 (1956).
70. Kuramotos, Y. & Kato, Y. Dynamics of One-Dimensional Quantum Systems: Inverse-Square Interaction Models. Cambridge. Univ. Press (2009).
71. Dong, S. H. *Wave Equations in Higher Dimensions*. Springer (2011).
72. Dong, S. H. *Factorization Method in Quantum Mechanics*. Springer (2007).
73. Landau, L. D. & Lifshitz, E. M. Quantum Mechanics, *Non-relativistic Theory* 3rd edition. Pergamon, Oxford (1977).
74. Sage, M. L. The vibrations and rotations of the pseudogaussian oscillator. *Chem. Phys* **87,** 431 (1984).
75. Sage, M. L. & Goodisman, J. Improving on the conventional presentation of molecular vibrations: Advantages of the pseudoharmonic potential and the direct construction of potential energy curves. *Am. J. Phys* **53,** 350 (1985).
76. Hurley, J. One-dimensional three-body problem. *J. Math. Phys* **8,** 813 (1967).
77. Calogero, F. Ground state of one-dimensional N body system. *J. Math. Phys* **10,** 2197 (1969).
78. Calogero, F. Solution of the one-dimensional N body problems with quadratic and/or inversely quadratic pair potentials. *J. Math. Phys.* **12,** 419 (1971).
79. Camiz, P., Gerardi, A., Marchioro, C., Presutti, E. & Scacciatelli, E. Exact solution of a time-dependent quantal harmonic oscillator with a singular perturbation. *J. Math. Phys.* **12,** 2040 (1971).
80. Dodonov, V. V., Malkin, I. A. & Man'ko, V. I. Green function and excitation of a singular oscillator. *Phys. Lett. A* **39,** 377 (1972).
81. Dong, S. H. & Ma, Z. Q. Algebraic Approach To The Pseudo-Harmonic Oscillator In 2D. *Int. J. Mod. Phys. E* **11,** 155 (2002).
82. Bayfield, J. E. *Quantum Evolution: An Introduction to Time-Dependent Quantum Mechanics* (New York: Wiley) (1999).
83. Alsing, P. & Zubairy, M. S. Collapse and revivals in a two-photon absorption process. *J. Opt. Soc. Am. B* **4,** 177 (1987).
84. Puri, R. R. & Bullough, R. K. Quantum electrodynamics of an atom making two-photon transitions in an ideal cavity. *J. Opt. Soc. Am. B* **5,** 2021 (1987).
85. Puri, R. R. & Agarwal, G. S. Collapse and revival phenomena in the Jaynes-Cummings model with cavity damping. *Phys. Rev. A* **33,** 3610(R) (1986).
86. Einstein, A., Podolsky, B. & Rosen, N. Can quantum mechanical description of physical reality be considered complete?. *Phys. Rev* **47,** 777 (1935).
87. Barenco, A., Deutsch, D., Ekert, A. & Jozsa, R. Conditional quantum dynamics and logic gates. *Phys. Rev. Lett* **74,** 4083 (1983).
88. Bengtsson, I. & Zyczkowski, K. Geometry of quantum states: An Introduction to Quantum Entanglement. Cambridge. Univ. Press (2006).
89. Zhou, L. & Sheng, Y. B. Detection of nonlocal atomic entanglement assisted by single photons. *Phys. Rev. A* **90,** 024301 (2014).
90. Bennett, C. H. *et al.* Teleporting an unknown quantum state via dual classical and Einstein-Podolsky-Rosen channels. *Phys. Rev. Lett* **70,** 1895 (1993).
91. Li, X. *et al.* Quantum Dense Coding Exploiting a Bright Einstein-Podolsky-Rosen Beam. *Phys. Rev. Lett* **88,** 047904 (2002).
92. Bennett, C. H. & Wiesner, S. J. Communication via one- and two-particle operators on Einstein-Podolsky-Rosen states. *Phys. Rev. Lett* **69,** 2881 (1992).
93. Ekert, A. K. Quantum cryptography based on Bell's theorem. *Phys. Rev. Lett* **67,** 6961 (1991).
94. Horodecki, R., Horodecki, P., Horodecki, M. & Horodecki, K. Quantum entanglement. *Rev. Mod. Phys* **81,** 865 (2009).
95. Wootters, W. K. Entanglement of formation of an arbitrary state of two qubits. *Phys. Rev. Lett* **80,** 2245 (1998).
96. Vidal, G. & Werner, R. F. Computable measure of entanglement. *Phys. Rev. A* **65,** 032314 (2002).
97. Vedral, V., Plenio, M. B., Jacobs, K. & Knight, P. L. Statistical inference, distinguishability of quantum states, and quantum entanglement. *Phys. Rev. A* **56,** 4452 (1997).
98. Walls, D. F. Squeezed states of light. *Nature* **306,** 141–146 (1983).
99. Wodkiewicz, K. & Eberly, J. H. Coherent states, squeezed fluctuations, and the SU(2) am SU(1,1) groups in quantum-optics applications. *J. Opt. Soc. Am. B* **2,** 458 (1985).
100. Buzek, V. *SU*(1, 1) squeezing of *SU*(1, 1) generalized coherent states. *J. Mod. Opt.* **37,** 303 (1990).

Acknowledgements

The authors would like to thank Professor M. K. Tavassoly for useful discussions and the referees as well as R. Lo Franco for their efficient and worthwhile suggestions to improve the presentation.

Author Contributions

A.D. conceived and designed the research. A.D. and B.M. performed the analysis and wrote the manuscript. S.S. and S.A. prepared all the figures.

Additional Information

Competing financial interests: The authors declare no competing financial interests.

How to cite this article: Dehghani, A. *et al.* Parity Deformed Jaynes-Cummings Model: "Robust Maximally Entangled States". *Sci. Rep.* **6**, 38069; doi: 10.1038/srep38069 (2016).

Publisher's note: Springer Nature remains neutral with regard to jurisdictional claims in published maps and institutional affiliations.